Electrochemistry of Iron(I) Porphyrins in the Presence of Carbon Monoxide. Comparison with Zinc Porphyrins

Gabriele Balducci,[1a] Geneviève Chottard,[1b] Claire Gueutin,[1c] Doris Lexa, and Jean-Michel Savéant*

Laboratoire d'Electrochimie Moléculaire de l'Université Denis Diderot, URA CNRS 438, 2 Place Jussieu, 75251 Paris Cedex 05, France

Received June 22, 1993®

As shown by combined use of cyclic voltammetry, thin-layer spectroelectrochemistry, UV–vis, and Raman spectroscopy of electrolyzed solutions, the presence of carbon monoxide as an axial ligand triggers the formation of the phlorin anion complexes upon reduction of iron(I) porphyrins at the expense of the corresponding iron("0") porphyrins. The presence of electron-withdrawing substituents on the phenyl groups of TPP, such as fluorine atoms, considerably slows down the protonation of the meso-carbon that yields the phlorin anion complex. The electrochemical properties of the phlorin anion complexes, investigated in the case where the metal is zinc, are also dependent upon the axial ligand, particularly CO. In the latter case, clear evidence of the stepwise character of the $-(2e^- + H^+)$ oxidation of the phlorin anion complex back to the parent porphyrin was obtained.

Introduction or removal of one electron from a metalloporphyrin may involve the orbitals of the ligand or those of the metal depending on structural factors such as the nature of the central metal and the presence of electron-withdrawing or -donating substituents on the porphyrin ligand.[2] Borderline situations may also exist in which the energies of the ligand and metal orbitals are close one to the other. In this connection, it is noteworthy that the distribution of the electron density over the porphyrin ligand and the metal may change with the axial ligand and thereof may be a function of the nature of the solvent. This change has been observed for example with chromium porphyrins that may exist under the form of chromium(II) or chromium(III) anion radical species.[3] Other examples, concerning the reduction and oxidation of nickel(II) porphyrins have been mentioned.[4]

The site of the electron introduction or removal is central to the chemistry that may ensue and is therefore of particular relevance to the design of catalytic cycles involving low- or high-valent metalloporphyrins. Localization of the extra electron or hole in the porphyrin ligand will trigger, in most cases, an irreversible destruction of the catalyst by reaction with the electrophile or nucleophile substrate. Conversely, metal-centered reductions or oxidations may allow the development of a catalytic cycle utilizing the coordination sphere of the metal.

In this framework, iron("0") porphyrins generated electrochemically from their iron(I) parents have been shown to undergo metal-centered reactions with alkyl monohalides,[5] vicinal dihalides,[6] and carbon dioxide,[7] leading in the two latter cases to an efficient catalysis of the corresponding electrochemical reactions. In the reaction of TPP $Fe^{"0"}$ with carbon dioxide, it is noteworthy that saturation of the ring takes place if the reaction of the metal is not competitively accelerated by the introduction of Lewis acids or by lowering the temperature.[7b] These observations indicate that the energies of the TPP ligand orbital and of that of the metal are not very different.

It has been shown that carbon monoxide strongly binds to iron(II) porphyrins but may also bind to iron(I) porphyrins. In the latter case, binding of CO is favored by the presence of an axial ligand and by NHCO substituents in the ortho position of the phenyl rings as in picket-fence and basket-handle superstructures.[8] It was then noted that the $Fe^{I}CO$ complex thus obtained exhibits a further cyclic voltammetric reduction wave. However this has not been assigned to a precise electrochemical reaction so far.

In the absence of CO as axial ligand, iron(I) porphyrins are reduced electrochemically into iron("0") complexes that are chemically stable in aprotic solvents such as DMF and DMSO within the time scale of slow scan cyclic voltammetry, thin-layer spectroelectrochemistry and even for longer time periods under careful exclusion of water and dioxygen. They are also electrochemically stable in the sense that no further reduction wave is found beyond the $Fe^{I}/Fe^{"0"}$ wave. Does the presence of carbon monoxide affect the acid–base and redox properties of the iron(I) porphyrin, so as to trigger a different chemistry, is the question that will be discussed in the following sections as an illustration of the possible role of axial ligands in modulating the chemistry of low-valent metalloporphyrins. Most of the experiments were carried out with the picket-fence porphyrin shown in Figure 1. The basket-handle porphyrin shown in Figure 1 and the tetrakis(pentafluorophenyl)porphyrin were investigated for comparative purposes.

In the course of this study, comparison with zinc(II) porphyrins that are known to give rise to phlorins upon $2e^- + H^+$ reduction[9] were found particularly enlightning. This was the occasion to further investigate the reduction and oxidation patterns of zinc

* Abstract published in *Advance ACS Abstracts*, March 15, 1994.

(1) (a) Present address: Dipartimento di Scienze Chimiche, 1 Via Licio Giorgieri, 34127 Trieste, Italy. (b) Laboratoire de Chimie des Métaux de Transition, Université Pierre et Marie Curie, Paris, France. (c) Present address: Laboratoire de Chimie Analytique, Université de Paris XI, Centre d'Etudes Pharmaceutiques, rue Jean-Batiste Clément, 92290 Châtenay Malabry, France.

(2) Kadish, K. M. *Iron-Porphyrins*; Gray, H. B., Ed.; Addison-Wesley: Reading, MA, 1983; Part II, pp 211–219.

(3) Guldi, D. M.; Hambright, P.; Lexa, D.; Neta, P.; Savéant, J.-M. *J. Phys. Chem.* **1992**, *96*, 4466.

(4) (a) Lexa, D.; Momenteau, M.; Mispelter, J.; Savéant, J.-M. *Inorg. Chem.* **1989**, *28*, 30. (b) Nahor, G. S.; Neta, P.; Hambright, P.; Robinson, L. R.; Harriman, A. *J. Phys. Chem.* **1990**, *94*, 6659. (c) Kadish, K. M.; Franzen, M. M.; Han, B. C.; Araullo-McAdams, C.; Sazou, D. *J. Am. Chem. Soc.* **1991**, *113*, 512.

(5) (a) Lexa, D.; Savéant, J.-M.; Wang, D. L. *Organometallics* **1986**, *5*, 1428. (b) Lexa, D.; Savéant, J.-M.; Su, K. B.; Wang, D. L. *J. Am. Chem. Soc.* **1988**, *110*, 7617. (c) Gueutin, C.; Lexa, D.; Wang, D. L.; Savéant, J.-M. *Organometallics* **1989**, *8*, 1607.

(6) Lexa, D.; Savéant, J.-M.; Schafer, H. J.; Su, K. B.; Vering, B.; Wang, D. L. *J. Am. Chem. Soc.* **1990**, *112*, 6162.

(7) (a) Hammouche, M.; Lexa, D.; Momenteau, M.; Savéant, J.-M. *J. Electroanal. Chem.* **1988**, *249*, 347. (b) Hammouche, M.; Lexa, D.; Momenteau, M.; Savéant, J.-M. *J. Am. Chem. Soc.* **1991**, *113*, 8455.

(8) Croisy, A.; Lexa, D.; Momenteau, M.; Savéant, J.-M. *Organometallics* **1985**, *9*, 1574.

(9) (a) Lanese, J. G.; Wilson, G. S. *J. Electrochem. Soc.* **1972**, *119*, 1039. (b) Closs, G. L.; Closs, L. E. *J. Am. Chem. Soc.* **1963**, *85*, 818. (c) Peychal-Heiling, G.; Wilson, G. S. *Anal. Chem.* **1971**, *43*, 545. (d) Peychal-Heiling, G.; Wilson, G. S. *Anal. Chem.* **1971**, *43*, 550.

0020-1669/94/1333-1972$04.50/0

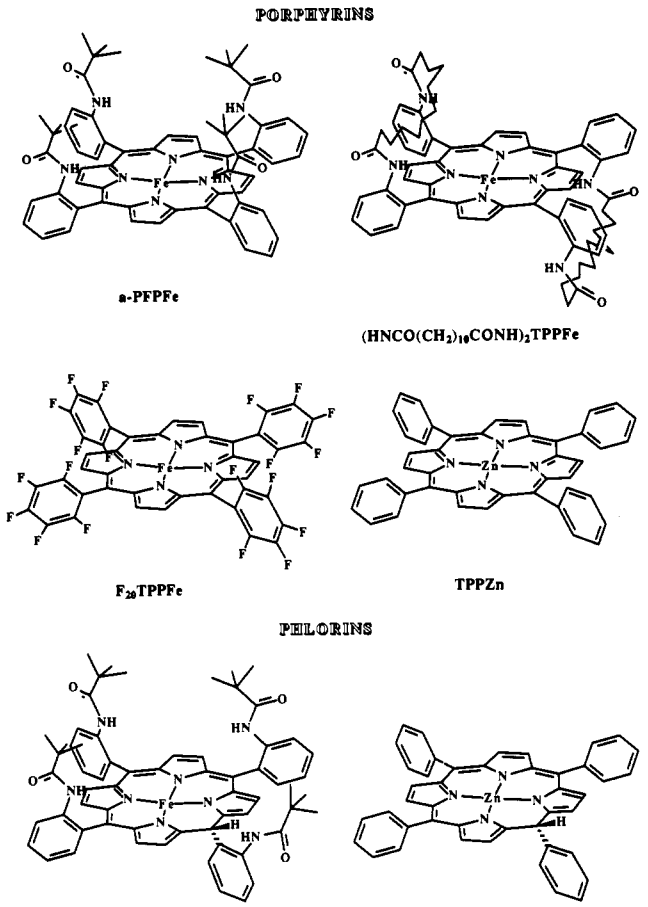

Figure 1. Porphyrins and phlorins investigated in this work.

phlorins and to show the role played by axial ligands (OH^-, CO) also in this case.

Results and Discussion

The cyclic voltammetry of a-PFPFe^{III}Cl in DMF, in the presence and absence of CO, is summarized in Figure 2. In the absence of CO, three successive reversible one-electron waves are observed, corresponding to the stepwise formation of the Fe^{II}, $(Fe^{I})^-$, and $(Fe^{"0"})^{2-}$ complexes. Under 1 atm CO and upon addition of *N*-methylimidazole aiming at stabilizing the Fe^{I}–CO adduct,[8] several changes are observed. The first, Fe^{III}/Fe^{II}, wave disappears because the strong relative stabilization of the Fe^{II} against the Fe^{III} complex, triggered by the binding of one CO molecule, induces the spontaneous reduction of the latter during the time where the electrode potential is poised at its initial value. The presence of CO shifts the remaining Fe^{II}/Fe^{I} wave toward negative values in line with a stronger CO binding at Fe^{II} than at Fe^{I}.[8] For a similar reason, the Fe^{I}/Fe$^{"0"}$ wave is also shifted toward negative values. In addition, a small reversible wave appears beyond the Fe^{I}/Fe$^{"0"}$ couple, the height of which increases upon decreasing the scan rate (Figure 2b,c). This observation points to the formation of a new complex resulting from the reduction of the CO–Fe^{I} porphyrin. Its presence is also revealed by an irreversible oxidation wave located around –0.45 V vs SCE. This new complex is formed by a relatively slow transformation of the CO–Fe^{I} reduction product as attested by the observation that its wave increases as the scan rate is decreased (Figure 2b,c) or when the starting potential is poised beyond the Fe^{I}/Fe$^{"0"}$ wave and the potential then scanned anodically (Figure 2d).

Thin-layer UV–vis spectroelectrochemistry (Figure 3) confirms the formation of the new complex. After electrolysis at –0.7 V (vs SCE) the Fe^{II}CO porphyrin is obtained as shown in Figure 3a (the same result could be obtained at potentials as positive as –0.1 V (vs SCE) albeit the production of Fe^{II}CO was slower).

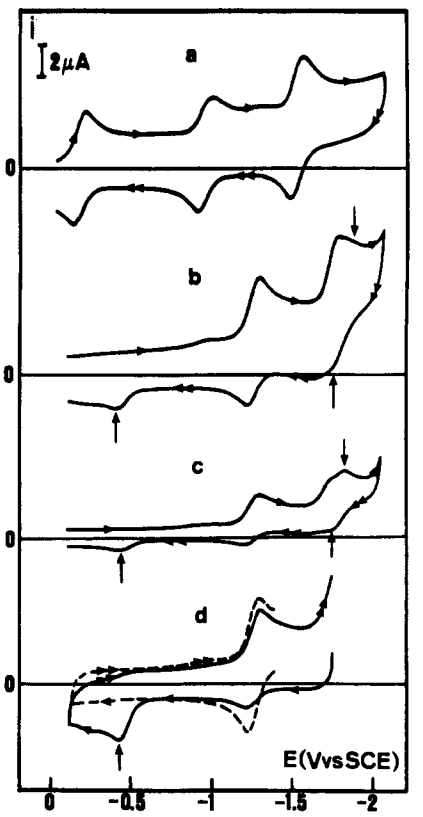

Figure 2. Cyclic voltammetry of a-PFPFe^{III}Cl (0.55 mM) in DMF + 0.1 M Et_4NClO_4 at 20 °C in the absence of CO (a) and in the presence of CO (1 atm) and of *N*-methylimidazole (0.1 M). Scan rates ($V \cdot s^{-1}$) were as follows: a, b, d, 0.1; c, 0.02. The vertical arrows indicate the waves resulting from the reduction and oxidation of the complex formed upon reduction of the CO–Fe^{I} porphyrin.

Further electrolysis at –1.35 V (vs SCE) produced the spectrum of the Fe^{I}CO complex (Figure 3b). The spectrum of the new complex appears upon electrolysis at –1.7 V (vs SCE). It exhibits two main bands, one in the Soret region, at 456 nm, $\epsilon = 58$ (mM^{-1} cm^{-1}), and the other in the near-infrared region, at 870 nm, $\epsilon = 10$ (see Table 1) and is clearly different from the spectrum of the iron("0") complex ($\lambda_{max} = 368$, $\epsilon_{max} = 56$; $\lambda_{max} = 468$, $\epsilon_{max} = 86$; $\lambda_{max} = 528$, $\epsilon_{max} = 32$).[10] As seen later on, the same spectrum is observed in the absence of *N*-methylimidazole, i.e., when the Fe^{I} porphyrin exists in the solution as a mixture of the carbonylated and non-carbonylated complexes.

Another interesting observation is that upon reoxidation at –0.2 V vs SCE of the new complex formed upon electrolysis at –1.70 V (vs SCE), the a-PFPFe^{II}(CO)(*N*-MeIm) is formed (the same spectrum as in Figure 3a is obtained). The electrochemical and UV–vis spectrochemical characteristics of the new complex thus suggest that it should be an iron(II) phlorin anion (Figure 1), formally deriving from the iron(II) porphyrin by a $2e^- + H^+$ reduction.

Phlorin anion complexes obtained from the $2e^- + H^+$ reduction of porphyrins[9c] have been investigated in particular details in the case where the metal is zinc.[9a] In DMF (with 0.1 M Et_4NClO_4 as supporting electrolyte). Zinc(II) tetraphenylporphyrin exhibits two one-electron reversible waves corresponding to the successive formation of the ring anion radical and dianion:[9a]

$$TPPZn^{II} + e^- \rightleftarrows {}^{\bullet-}TPPZn^{II} \qquad E^0 = -1.34 \text{ V (vs SCE)}$$

$$^{\bullet-}TPPZn^{II} + e^- \rightleftarrows {}^{2-}TPPZn^{II} \qquad E_0 = -1.74 \text{ V (vs SCE)}$$

The dianion thus produced is not stable in the time scale of thin-

(10) Anxolabéhère, E.; Chottard, G.; Lexa, D. Submitted.

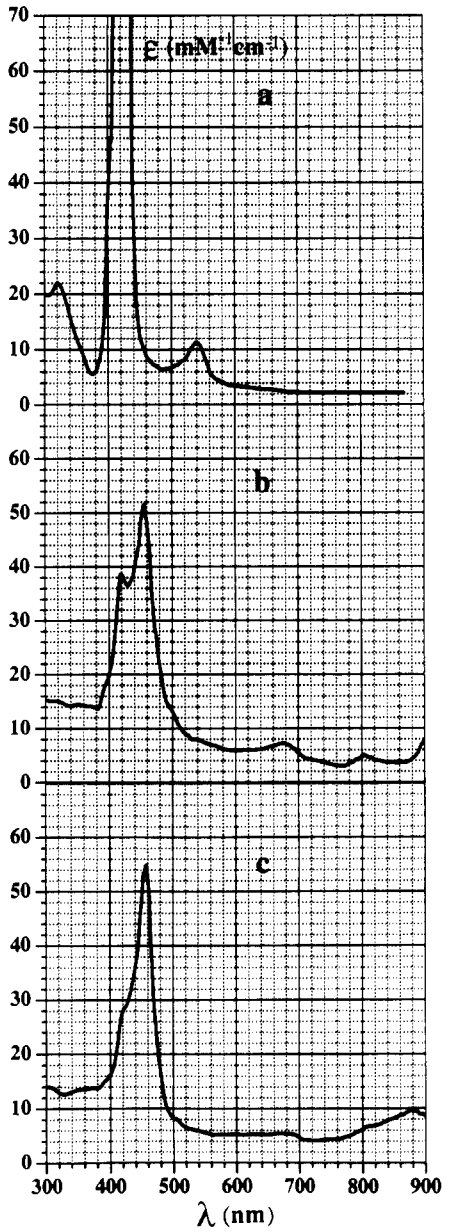

Figure 3. Spectroelectrochemistry of a-PFPFeCl (0.18 mM) in DMF (+0.1 M Et_4NClO_4) in the presence of 1 atm CO and of *N*-methylimidazole (30 mM): a, $Fe^{II}CO$ obtained by electrolysis at −0.7 V (vs SCE); b, $Fe^{I}CO$ obtained by further electrolysis at −1.35 V (vs SCE); c, further electrolysis at −1.70 V (vs SCE).

layer spectroelectrochemistry. It accepts one proton from the reaction medium which binds to one of the meso-carbons, then leading to the phlorin anion complex (Figure 1)

$$^{2-}TPPZn^{II} + H^+ \rightleftarrows {}^{-}TPHPhlZn^{II}$$

that can be identified by means of its UV–vis spectrum (Figure 4a). The spectrum thus obtained conforms to the spectra previously obtained by means of spectroelectrochemistry[9a] or chemical reduction.[9b] Similar spectra were obtained in butyronitrile and in DMSO (Table 1).

The strong similarity between the spectrum of $^{-}$TPHPhlZn and that obtained by the two-electron reduction of a-$PFPFe^{II}$ (Figure 4) is a first indication that the iron complex thus obtained is the iron(II) phlorin anion complex.

This assignment is confirmed by the similarity between the cyclic voltammogram of $^{-}$TPHPhlZn and that of the iron complex obtained upon electrolysis of the a-PFPFe porphyrin at −1.60 V (vs SCE) (Figure 5). The latter gives back the porphyrin upon

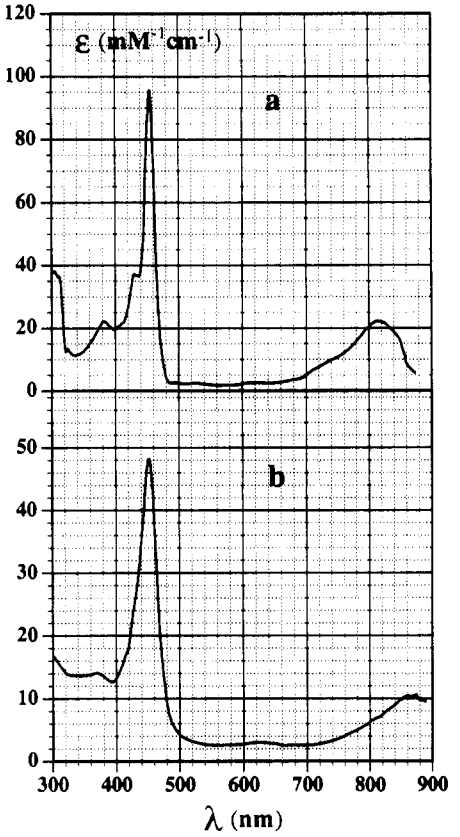

Figure 4. (a) UV–vis spectrum of $^{-}$TPHPhlZn obtained by preparative-scale electrolysis of a 0.54 mM solution of TPPZn at −1.8 V (vs SCE) under a dry argon atmosphere (glovebox). (b) Thin-layer UV–vis spectroelectrochemistry of the reduction of a-PFPFe (0.11 mM) at −1.6 V (vs SCE) under a 1 atm CO atmosphere. Solvent was DMF (+0.1 M Et_4NClO_4).

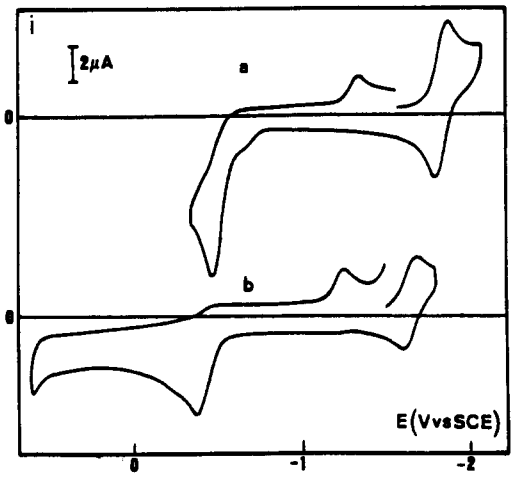

Figure 5. Cyclic voltammograms after preparative-scale electrolysis of TPPZn (0.5 mM) at −1.80 V (vs SCE) in a dry argon atmosphere (a) and of a-PFPFeCl (0.65 mM) at −1.60 V (vs SCE) under a 1 atm CO atmosphere. Solvent was DMF (+ 0.1 M Et_4NClO_4). Scan rate was 0.1 V/s.

a two-electron irreversible oxidation as seen in Figure 5b and already found in spectroelectrochemistry. This is also the case for $^{-}$TPHPhlZn (Figure 5a).[9a] The characteristic reduction and oxidation potentials are listed in Table 2.

A final confirmation of the nature of the iron complex was provided by Raman spectroscopic analysis of the electrolyzed solutions. As seen in Figure 6 and Table 1, the Raman spectra of $^{-}$TPHPhlZn and of the iron complex are very similar. In both cases, there is a very strong ν_4 band at 1345 and 1352 cm^{-1}, a doubled ν_1 band, and a ν_6 band around 1020 cm^{-1}. The ν_1 doublet

Table 1. UV–Vis and Resonance Raman Characteristics of the Phlorin Anion Complexes

starting porphyrin	electrolysis conditions for the generation of the phlorin complex: solvent (atmosphere)	potential (V vs SCE)	spectral characteristics: UV–vis λ_{max} (nm) (ϵ (mM^{-1} cm^{-1}))	low frequency Raman bands ν (cm^{-1})
a-PFPFE^{II}	DMF (CO)	−1.60	452 870[a] (49) (11)	838 w[c,e] 707 w 437 w
	DMF (CO)	−1.60	456 874[a,b] (58) (10)	
$(NH\text{-}CO\text{-}(CH_2)_{10}\text{-}CO\text{-}NH)_2TPPFe^{II}$	DMF (CO)	−1.50	458 870[a,b] (51) (10)	838 m[c,e] 706 m 431 m
TPPZn	DMF (Ar)	−1.75	454 814[c,d] (96) (22)	
	DMF (CO)	−1.75	454 814[c,d] (96) (22)	
	DMSO (Ar)	−1.70	456 824[a] (70) (19)	
	DMSO (CO)	−1.75	456 825[a,c] (79) (22)	840 w[c,e] 705 w 434 s
	PrCN (Ar)	−1.75	458 824[c,d] (83) (25)	
	PrCN(CO)	−1.75	452 808[c,d] (80) (19)	

[a] Spectroelectrochemistry. [b] In the presence of *N*-methylimidazole. [c] Recorded after preparative-scale electrolysis (two-electron reduction of TPPZn, a-PFPFe^{II}, or $(NH\text{-}CO\text{-}(CH_2)_{10}\text{-}CO\text{-}NH)32TPPFe^{II}$) and transfer in the spectrochemical cell (see Experimental Section). [d] Electrolysis carried out in the glove box. [e] Key: m, medium intensity; s, strong intensity; w, weak intensity.

Table 2. Characteristic Potentials (V vs SCE(of the Phlorin Anion Complexes

starting porphyrin	electrolysis conditions for the generation of the phlorin complex: solvent (atmosphere)		potential (V vs SCE)	characteristic potentials[a]: reduction E^0 [b]	oxidation Ep_a[c]
a-PFPFe^{II}	DMF	(CO)[d]	−1.60	−1.75	−0.37[f]
$(NH\text{-}CO\text{-}(CH_2)_{10}\text{-}CO\text{-}NH)_2TPPFe^{II}$	DMF	(CO)[d]	−1.50	−1.62	−0.40[f]
TPPZn	DMF	(Ar)[e]	−1.75	−1.91	−0.55
		(CO)[e]	−1.75	−1.89	−0.54
	DMSO	(Ar)[d]	−1.70	−1.80	−0.44
		(CO)[d]		−1.80	−0.41
	PrCN	(Ar)[e]	−1.75	two waves[g]	two waves −0.59 −0.81
		(CO)[e]	−1.75	two waves[h] −1.99	−0.76

[a] Measured on voltammograms after preparative scale electrolysis (two-electron reduction of TPPZn, a-PFPFe^{II}, or $(NH\text{-}CO\text{-}(CH_2)_{10}\text{-}CO\text{-}NH)_2TPPFe^{II}$). [b] Formal potential obtained as the midpoint between the cathodic and anodic peak potentials. [c] Anodic peak potential at 0.1 $V{\cdot}s^{-1}$. [d] Out of the glove box. [e] In the glovebox. [f] Peak potential of the highest wave. [g] E^0 cannot be measured. [h] E^0 of the highest wave.

is quite characteristic of $^-$TPHPhlZn, but in the a-PFPFe case, there is already a doubling of the band due the ortho-substitution of the phenyl groups. In the low-frequency region, the similarity of all the observed bands points to the similarity of the two structures.[11]

We may thus conclude at this stage that the presence of CO as an axial ligand in iron(I) porphyrins induces a change in the reduction mechanism as summarized in Scheme 1 in which, for clarity, only the main resonant forms are figured. By analogy with previously investigated reaction schemes,[12] it is easy to see that the height of the reduction wave of the iron(II) phlorin anion complex is predicted to be an increasing function of the parameter $(K[CO]k/v)$ (RT/F), where v is the scan rate. This explains why the height of this wave increases as the scan rate is decreased (Figure 2). The height of its oxidation wave also increases as the scan rate decreases and also if the starting potential is poised beyond the reduction wave of the porphyrin: more time is then provided for the production of the iron phlorin anion complex.

Quite similar results were obtained with another modified iron TPP porphyrin also bearing NHCO functions in the ortho positions of the phenyl rings, namely, the basket-handle porphyrin shown in Figure 1.

In contrast, with the perfluoro-TPP porphyrin (Figure 1), even in the presence of *N*-methylimidazole, no reduction wave following the reduction wave of the iron(I) complex under 1 atm CO and no oxidation wave on the reverse scan could be detected. Thin-layer spectroelectrochemistry showed that the reduction of a mixture of the carbonylated and non-carbonylated iron(I) complexes leads to the iron("0") porphyrins with no trace of the formation of a phlorin anion complex (Figure 7).

The most likely explanation of this difference in behavior between the two types of porphyrins is that, in the case of the perfluoroporphyrin, part of the negative charge is shifted toward the pentafluorophenyl rings leaving insufficient charge density on meso positions of the porphyrin ring for protonation to occur.

The role of CO axial binding favoring the formation of the phlorin anion complex during the reduction of iron(I) porphyrins may be rationalized as follows. It is well-known, as recalled earlier, that CO has a particularly strong affinity for iron(II) in porphyrin complexes, much stronger than for the corresponding

(11) (a) The Raman spectrum of $^-$HPhlZn shown in Figure 6 is very similar to that of $^-$HPhlMg previously reported in the literature. (b) Yamaguchi, H.; Soeta, A.; Toeda, H.; Itoh, K. *J. Electroanal. Chem.* **1983**, *159*, 347.

(12) Andrieux, C. P.; Savéant, J.-M. Electrochemical Reactions *In Investigation of Rates and Mechanisms of Reactions, Techniques of Chemistry*; Bernasconi, C. F., Ed.; Wiley: New York, 1986; Vol. VI/4E, Part 2, pp 305–390.

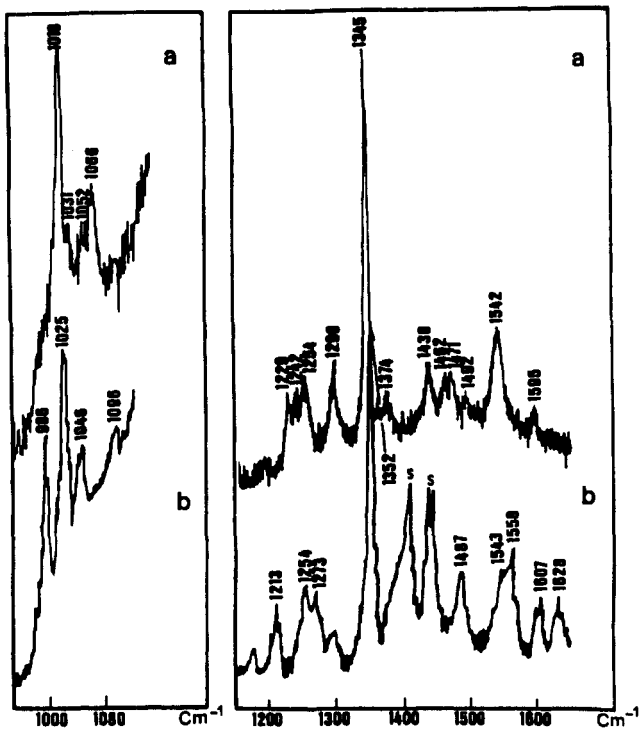

Figure 6. (a) Raman spectroscopy at medium and high frequencies of $^{-}$TPHPhlZn obtained by electrolysis at −1.70 V (vs SCE) of a 0.9 mM solution of TPPZn in DMSO under 1 atm. CO. (b) Product of electrolysis at −1.60 V (vs SCE) of a 0.60 mM solution of a-PFPFeCl solution in DMF under 1 atm of CO.

Scheme 1

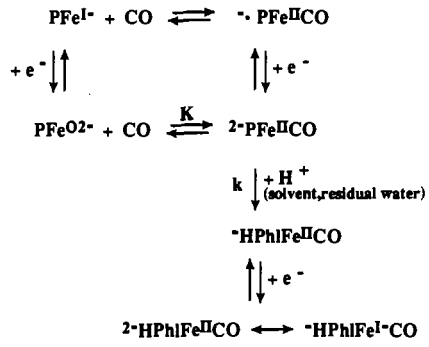

iron(III) and iron(I) complexes. As a consequence, in the carbonylated iron ("I") and iron("0") complexes, much of the negative charge is transferred from the metal to the ring so as to restore the privileged $Fe^{II}CO$ binding. In the latter case, enough negative charge, with the already noted exception of perfluoro-TPP, is thus present on the meso-carbons so as to trigger the protonation of one of them.

As seen above, the oxidation wave of the iron and zinc phlorin anion complexes has been a useful clue in the identification of the species formed upon reduction of carbonylated iron porphyrins. In the course of this study we have found that the mechanism of the oxidation of the zinc phlorin is somewhat more complex than described earlier[9a] and may depend upon the nature of the axial ligand of the metal atom.

The most significant variations were observed when butyronitrile (PrCN) was the solvent. In this solvent, as well as in DMF and DMSO, the first wave for the reduction of the zinc porphyrin in the corresponding anion radical is reversible when argon U is used for purging the solution from dioxygen and to protect the solution from dioxygen during the experiment. The same is true for thin-layer UV–vis spectroelectrochemistry. However, the anion radical is not stable when produced by preparative-scale electrolysis under the same conditions. The production of a stable

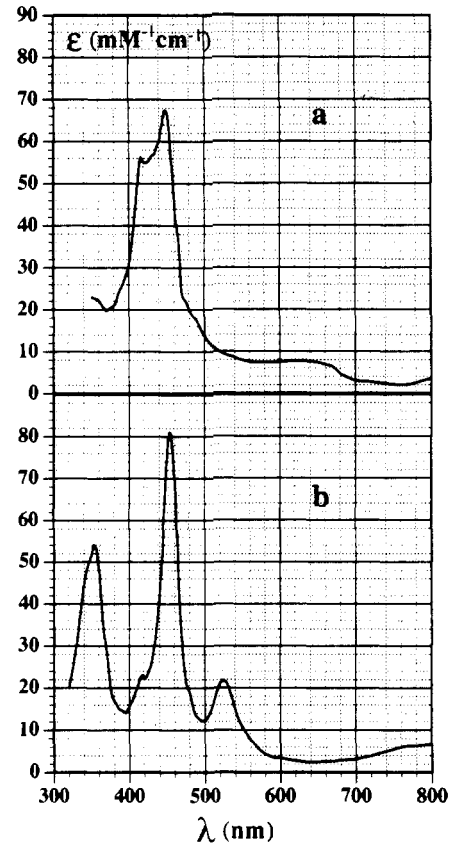

Figure 7. Thin-layer UV–vis spectroelectrochemistry of the reduction of $F_{20}TPPFeCl$ (0.21 mM) in DMF (+0.1 M Et_4NClO_4) in the presence of 1 atm of CO and 20 mM *N*-methylimidazole at −1.40 (a) and −1.70 (b) V (vs SCE).

anion radical requires that argon C be used instead of argon U, or that electrolysis be carried out in a glovebox under pre-deoxygenated and pre-dried argon. With one or the other of these two procedures we could investigate the formation of the phlorin by protonation of dianion of the zinc porphyrins generated at a more negative potential.

However, as seen in Figure 8, the cyclic voltammetry behaviors of the phlorin anion complex obtained by one or the other of these two procedures in PrCN are not the same. When the phlorin anion complex was prepared in the glovebox, the electrolysis consumed two electrons per molecule and all the porphyrin was transformed (Figure 8a). Outside the glovebox even using a flux of the best grade argon (C) over the solution during electrolysis, not all the porphyrin was transformed (Figure 8b) in spite of a larger consumption of electricity (2.5 electrons per molecule). With the first procedure, the two-electron oxidation of the phlorin anion complex is split into two close-spaced waves whereas, with the second procedure, a single oxidation wave is observed at the same potential as that of the less positive of the two previous waves. These observations suggest that the base, presumably OH^- from residual water, generated during the reductive conversion of the zinc porphyrin into the phlorin anion complex (that consumes 1 H^+ per molecule) acts as an axial ligand in competition with the solvent. Because of the strong electron-donating power of this axial ligand, the resulting complex is easier to oxidize than the complex where the metal is axially ligated by a solvent molecule. Their oxidation thus takes place at the first and second waves respectively in the case where the synthesis of the phlorin anion complex was carried out in the glovebox. With the second procedure, more OH^- is generated during the preparative electrolysis, through reduction of trace dioxygen continuously present in the argon flux. This explains that the first wave then predominates over the second.

We also note (Figure 8a) that, with the glovebox procedure,

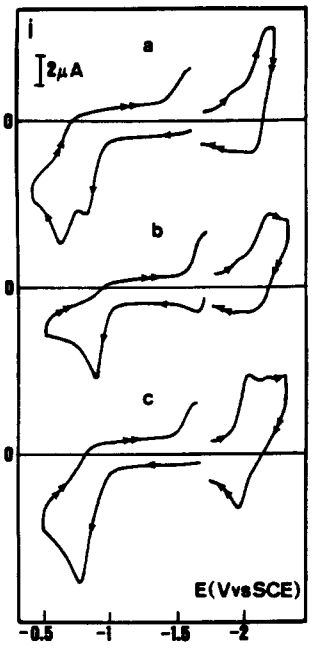

Figure 8. Cyclic voltammetry of $^{-}$TPHPhlZn^{II} in PrCN (+ 0.1 M Et_4NClO_4) prepared by electrolysis of TPPZn^{II} at −1.75 V (vs SCE): scan rate, 0.1 V/s; initial concentration of TPPZn^{II}, 0.51 mM (a, c), 0.41 mM (b); under argon in a glovebox ($(O_2 \approx 4$ ppm) (a), under argon C outside of the glovebox (b), under 1 atm of CO in the glovebox (c).

the reduction of the phlorin anion complex is also split in two waves, the less negative wave being smaller than the successive wave whereas, on the oxidation side, the less positive wave was higher than the successive wave. These observations may be explained within the same framework, noting that the complex axially ligated by OH^- is more difficult to reduce than the complex bearing a solvent molecule as axial ligand whereas the order of oxidability is reversed. With the second procedure, two reduction waves also appear, but the first of them corresponds to the second reduction wave of the residual zinc porphyrin rather than to the reduction of the phlorin complex. In this case, both the oxidation and the reduction of the phlorin anion complex involve the OH^- ligated complex.

The presence of carbon monoxide also modifies both the oxidation and reduction patterns of the phlorin anion complex. As seen in Figure 8c, the split oxidation wave is replaced by a single wave, the peak potential of which is located between those of the OH^- and solvent complexes. On the reduction side, the less negative wave now largely predominates over the successive wave, the first reduction wave being also located between those of the OH^- and solvent complex. We may interpret these observation as pointing to the formation of a phlorin anion complex axially ligated by one molecule of CO. As expected, its oxidation is more difficult than that of the OH^- complex and easier than that of the solvent complex and vice versa for the reduction.

The axial complexation by OH^- or CO in PrCN also appears in the UV–vis spectra obtained after electrolysis in the zinc porphyrin in a glovebox (Table 1): a small but distinct bathochromic shift of the two main bands is observed between the second and the first complex in keeping with their electrochemical characteristics.

In DMF and DMSO, the cyclic voltammograms are much less affected by the presence of OH^- than in PrCN, presumably because the molecules of these solvents are much better ligands of the metal. The UV–vis spectra do not reveal a significant effect of the presence of CO (Table 1). However, significant differences appear in the cyclic voltammograms (Figure 9). In DMSO, the oxidation peak is slightly more positive in the presence than in the absence of CO suggesting that CO has replaced DMSO as axial ligand even though the properties of the two complexes

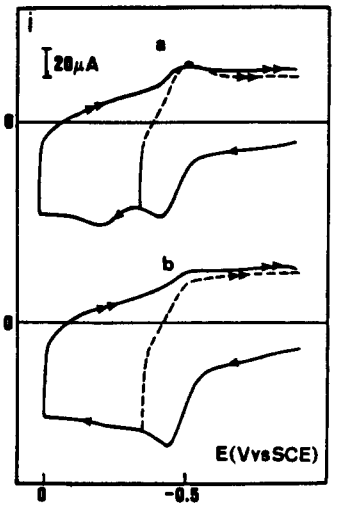

Figure 9. Cyclic voltammetry of $^{-}$TPHPhlZn^{II} in DMSO (+0.1 M Et_4NClO_4) prepared by electrolysis of a 1 mM solution of TPPZn^{II} at −1.7 V (vs SCE) under an argon C atmosphere after (a) and before (b) saturation of the solution by CO. Scan rate was 10 V/s.

are not very different (as are the UV–vis spectral properties). This is confirmed by a different evolution of the cyclic voltammetric patterns upon raising the scan rate.

It is noted that the single two-electron oxidation wave tends to split into two waves and that the first of these tends to become reversible. It is seen (Figure 9) that this evolution appears at lower scan rates for the CO complex than for the DMSO complex.

Unlike previous observations,[9a] this makes clear that the oxidation of the phlorin anion complex involves two successive one-electron transfers separated by the removal of a proton according to an ECE–DISP mechanism[12]

$$^{-}\text{HPhlZn}^{II} - e^- \rightleftarrows {}^{\bullet}\text{HPhlZn}^{II}$$

$$^{\bullet}\text{HPhlZn}^{II} \rightleftarrows H^+ + {}^{-\bullet}\text{PorphZn}^{II}$$

$$^{-\bullet}\text{PorphZn}^{II} - e^- \rightleftarrows \text{PorphZn}^{II}\ \text{(ECE)}$$

and/or

$$^{\bullet}\text{HPhlZn}^{II} + {}^{-\bullet}\text{PorphZn}^{II} \rightleftarrows {}^{-}\text{HPhlZn}^{II} + \text{PorphZn}^{II}\ \text{(DISP)}$$

at the first wave[13] whereas, at the second wave, that appears upon raising the scan rate, proton abstraction takes place after the removal of a second electron (according to an "EEC" mechanism)

$$^{\bullet}\text{HPhlZn}^{II} - e^- \rightleftarrows {}^{+}\text{HPhlZn}^{II}$$

$$^{+}\text{HPhlZn} \rightleftarrows H^+ + \text{PorphZn}^{II}$$

The deprotonation of $^{\bullet}$HPhZn^{II} is slowed down by the presence of CO, presumably because its binding to the metal decreases the amount of positive charge on the phlorin ring and particularly at the saturated meso carbon from which the proton departs as the porphyrin ring is formed.

Conclusions

The main conclusion to emerge from the preceding results is that axial binding of carbon monoxide onto iron(I) porphyrins induces the charge density introduced by the uptake of an electron to be mostly located on the porphyrin ring. The resulting complex may consequently be protonated at one of the meso-carbons thus generating the iron(II) phlorin anion complex. The latter may

(13) In view of the relative slowness of the depronation reaction, the DISP pathway is likely to overrun the ECE pathway.[12]

be converted back to the iron(II) porphyrin upon anodic reoxidation. The propensity of the reduced $Fe^{I}CO$ porphyrins to protonate at one of the meso carbons is a function of the nature of the porphyrin ring: whereas the formation of the phlorin anion complex is observed with TPP porphyrins bearing NHCO functionalities in the ortho position of the phenyl rings, it does not take place when each phenyl ring is perfluorinated.

The electrochemical properties of phlorin anion complexes, as investigated with the zinc complex of the phlorin anion deriving from TPP, also depend upon the nature of the axial ligand. It is remarkable that axial ligation by CO allows one to observe the stepwise character of the $-2e^- - H^+$ oxidation of the phlorin anion complex into the parent porphyrin.

Experimental Section

Chemicals. Porphyrins: ZnTPP was from commercial origin (Aldrich, chlorin-free). a-$PFPFe^{III}Cl$ and $(NH\text{-}CO\text{-}(CH_2)_{10}\text{-}CO\text{-}NH)_2TPPFe^{III}Cl$ were provided by M. Momenteau. They were synthesized and characterized as described in ref 14.

N-Methylimidazole, from commercial origin (Aldrich, 99+%), was used as received.

Solvents and Electrolyte: All the solvents were from commercial origin. DMF and DMSO (Burdick & Jackson) were used as received. PrCN (Aldrich, 98%) was purified as described in ref 15. NEt_4ClO_4 (Fluka purum) was used as supporting electrolyte. It was recrystallized twice before use in a 1:2 ethyl acetate–95° ethanol mixture.

Cyclic Voltammetry. The cell and instrumentation were the same as previously described.[7] The solutions were degassed with argon U (O_2 <10 ppm) or C (O_2 < 3 ppm, H_2O < 3 ppm) or with CO (N47 grade, O_2 < 3 ppm, H_2O < 3 ppm). The working electrode was a 3 mm diameter glassy carbon disk. All potentials are referred to the aqueous NaCl saturated calomel electrode (SCE) in DMF and DMSO and to the Ag/Ag^+ ($AgClO_4$ 10^{-2} M in PrCN) electrode in PrCN ($E^0_{SCE} - E^0_{Ag/Ag^+} = -0.280$ V).

Preparative-Scale Electrolyses. The instrumentation was the same as previously described.[16] The reference electrodes were $Cd(Hg)/CdCl_2$ (saturated solution) in DMF,[17] SCE in DMSO, and Ag/Ag^+ in PrCN.

Spectroscopy. UV–vis spectra were recorded on a Varian (Cary 2200) spectrophotometer. They were obtained either from thin-layer spectroelectrochemistry experiments or after transfer of preparative electrolysis solutions in a degassed spectroscopic cell under an argon or CO stream. In the former case, the cell was the same as previously described[18] (optical length 0.05 cm), in the latter, it was a standard UV–vis cell (optical length 0.1 cm).

Resonance Raman spectra were recorded on a Jobin Yvon double monochromator U1000 equipped with a As Ga photomultiplier and a photocounting detector. The spectral width was 6 cm^{-1}. The exciting line was the 457.9-nm line of a Ar^+ laser at 20 mW incident power level. After electrolysis, the phlorin anion solutions were transferred in a degassed rotated cell (optical length 0.1 cm) under a argon or CO stream.

Acknowledgment. We are indebted to Michel Momenteau (Institut Curie, Orsay, France) for the gift of samples of the iron picket-fence and basket-handle porphyrins used in this work.

(14) (a) Collman, J. P.; Gagne, R. R.; Halbert, T. R.; Marchon, J. C.; Reed, C. A. *J. Am. Chem. Soc.* **1973**, *93*, 7868. (b) Momenteau, M.; Mispelter, J.; Loock, B.; Lhoste, J.-M. *J. Chem. Soc., Perkins Trans. 1* **1985**, 221. (c) Momenteau, M.; Loock, B. *J. Mol. Catal.* **1980**, *7*, 315.
(15) Van Duyne, R.; Reilley, C. N. *Anal. Chem.* **1972**, *44*, 142.
(16) Gueutin, C.; Lexa, D.; Momenteau, M.; Savéant, J.-M. *J. Am. Chem. Soc.* **1990**, *112*, 1874.
(17) Marple, L. W. *Anal. Chem.* **1967**, *39*, 86.
(18) Lexa, D.; Savéant, J.-M.; Zickler, J. *J. Am. Chem. Soc.* **1977**, *99*, 2786.